High-resolution vibroacoustic measurement and analysis of the DLR ISTAR aircraft to assess engine-induced cabin noise

René Winter[1], Julian Sinske[2], Marco Norambuena[3], Sebastian Zettel[4]

German Aerospace Center (DLR)
Institute of Aeroelasticity
Bunsenstraße 10
37073 Göttingen

ABSTRACT

Aircraft engines, especially when mounted directly to the fuselage, inject a considerable amount of tonal vibrations into the airframe causing audible and comfort reducing cabin noise. Reducing this noise requires the development of specialised noise reduction systems. This is a time consuming and expensive endeavour. To speed up and ease this process a sufficiently detailed numerical model of the aircraft structure and the force injected by the engines is required. The DLR ISTAR, a Dassault Falcon 2000LX, was used for an extensive vibration measurement campaign. The goal of this campaign was twofold: Getting spatially dense information about the aircrafts vibro-acoustic behaviour to later update a finite element model for calculations in the mid-frequency range and to analyse the vibration injected by running engines into the fuselage structure. The measurements include the vibration response to both shaker excitation and engine vibration of the DLR ISTAR at about 1300 positions acquired by a rowing grid of sensors. The results are presented in the form of operational deflection shapes and first calculations of energy transfer paths using structural intensity analysis.

1. INTRODUCTION

To understanding the transfer path of vibrations introduced into an airframe by distinct, sometimes tonal, vibration sources in the audible frequency range is a complicated task. The fuselage of an aircraft is build in a grid-like structure, with longitudinal stringers and circumferential frames keeping the skin layer in place. This creates a mesh of possible paths for the vibration energy to travel along.

To get a better understanding of the problem and to test possible solutions the German Aerospace Center (DLR), in cooperation with Dassault Aviation, conducted a large scale vibroacoustic measurement campaign on a research aircraft in march 2022. The aircraft in question was a Dassault Falcon 2000LX owned by DLR known as the ISTAR, an acronym for In-Flight Systems & Technology Airborne Research (see figure 1). The ISTAR is fitted with two rear mounted engines. Identifying

[1]rene.winter@dlr.de

[2]julian.sinske@dlr.de

[3]marco.norambuena@dlr.de

[4]sebastian.zettel@dlr.de

the vibration transfer originating at these engines to the passenger cabin is one of the goals of the project the presented work is part of. To get good results when using experimental structure intensity (STI) estimation for vibration transfer path analysis a sensor grid of high density is a necessity. In fact, higher the grid density the better [1].

To achieve a maximum number of measurement positions with a limited amount of sensors a rowing grid method [2, 3] is used. This process subdivides the planed grid into subgrids which are sequentially measured. The results are later merged into a full data set. DLR used this method several times already and proofed it works well for the repeatable artificial excitation of electromagnetic shakers.

The test campaign was conducted by DLR's vibration testing team over the course of two weeks, where the vibration response of the fuselage structure was measured at 1310 individual sensor positions on the fuselage alone. Additional sensors were deployed to the pressure bulk head and the cabin floor.

Figure 1: The DLR ISTAR with sensor configuration C1 installed. The full measurement grid is marked on the fuselage by removable stickers. © 2022 DLR

The engines and the forces injected by the engines are one primary focuses of the campaign, being one of the aforementioned tonal vibration sources. It was, however, not feasible to measure the whole fuselage structure with the full detailed grid of over 1300 accelerometer positions at once due to the limited availability of measurement system channels and sensors. Using a rowing grid method wasn't a possibility either due to long installation times caused by sensor and cable attachment requirements when measuring with running engines. A specific subset of the full grid was used for the engine runs focused on the fuselage response in the direct vicinity of the engines with a limited amount of sensors spread over the full length of the fuselage.

The acquired data was processed into the frequency domain to get operational deflection shapes during the test and afterwards further processed to acquire STI estimations.

2. METHODS

2.1. Vibroacoustic Testing - Equipment and Methods

As stated above, the test used methods previously developed for high density grid measurements of full scale aircraft structures. A detailed overview of the rowing grid testing process applied can be found in [2]. At it's core the process subdivides the measurement grid into subsections optimized to utilize as many sensors as possible at once while also allowing for an easy installation of the subsection and subsequent grid configurations. The specifics of the subgrids depend on the accessibility on site,

the available space for cable routing etc. This test posed the additional complication of an installation to the outside of an already painted aircraft, making the precise localisation of sensor positions very difficult and time consuming.

The Falcon 2000LX's relevant characteristics to sensor grid design for this project are: It has rear mounted engines, is 20.2 m long and has a cabin width of 2.35 m. Starting from these, the sensor grid was designed with several goals in mind: An existing finite elements model of the aircraft needs to be verified, updated and, especially for the fuselage section, refined for the higher frequency range. In addition the data will be used to calculate structural intensities (see section 2) to get an impression of the vibration energy flow through the fuselage. This energy flow should be considered both for artificial shaker excitation and operational vibrations caused by the engines. Within the scope of the projects time frame and the aircrafts accessibility these goals could only be reached by compromising on some of them. It was decided to not use more than five subgrids of up to 300 sensors each, as more subgrids would most likely not be doable in the scheduled time and more sensors in parallel would exceed the limits of what was available.

The base line finite element model (FEM) of the ISTAR is a symmetric model derived from a half-shell model. While this is not perfectly true for the actual aircraft it is sufficiently so in the rear half. Thus the detailed measurements were limited to one half of the aircraft assuming symmetry. With these limits established a measurement grid was designed using 1310 positions (see 2a) spread over five sensor configurations. In addition a limited amount of sensors used for verification purposes was installed on the other side of the aircraft (see figure 2b).

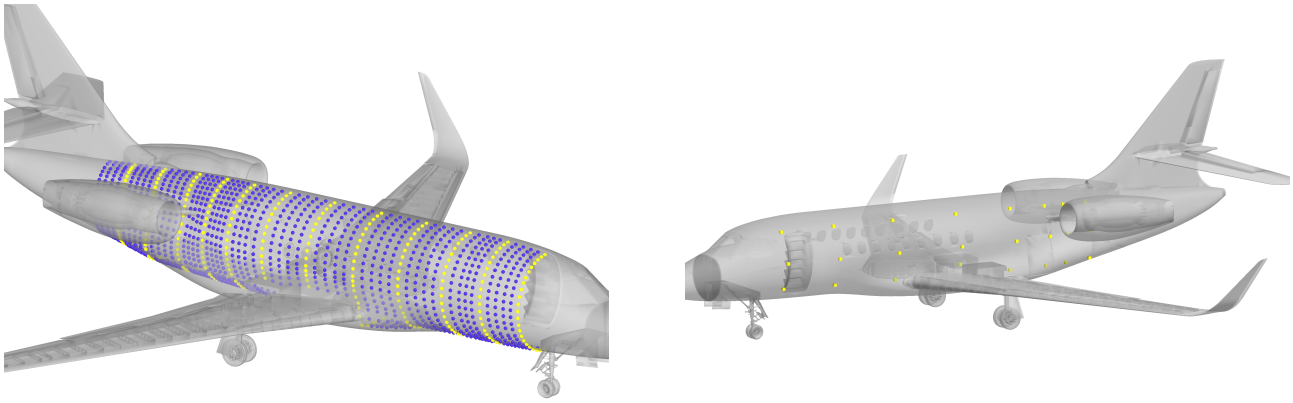

(a) C1 in yellow. C2-5 in blue

(b) sensors on left side.

Figure 2: Sensor configurations used during the test. The main test was done using 5 configurations C1 to C5 which wore installed and measured sequentially (see figure 2a). 24 sensors were permanently installed to the left side of the ISTAR (see figure 2b).

While previous measurements using sensors [3] used 15 sensors per skin field and surrounding stiffeners this measurement is limited to 6 sensors per equivalent structure. This will of course limit the frequency up to which reliable information can be gathered from the data, but otherwise the goal of having data along most of the fuselage would not have been reached. The measurement of the operational excitation by the engines caused a different problem: The rowing grid method was not a viable option as the installation time per configuration escalates. The sensors and their cables have to be secured so as to not being sucked into the engines. The aircraft has to be outside for the test. Depending on the weather that's not always an option. It was decided to only measure a single configuration with running engines. This configuration is focused on the area around the pylon, to get a good understanding of the vibrations injected into the aircraft (see figure 3a).

The vibroacoustic testing was conducted using accelorometers as sensors and electromagnetic shakers for artificial excitation. Specifically Kistler 8000M095 sensors were used. These have a viable frequency range of 0.5 Hz to 1 kHz and their casing and sensor elements were selected for optimal

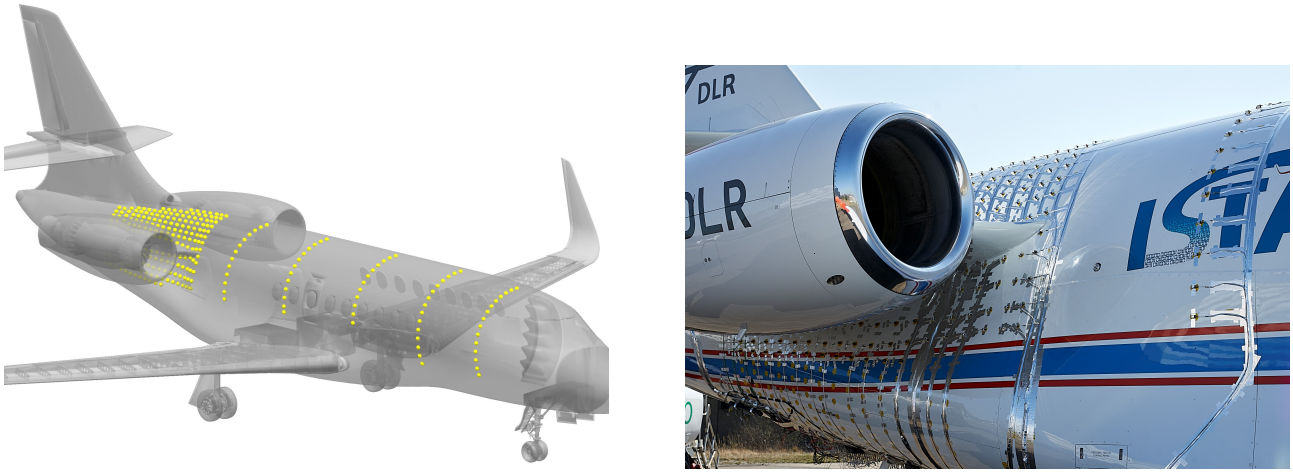

(a) Engine configuration plan

(b) Engine configuration realized © 2022 DLR

Figure 3: Sensor configuration used for the engine test. The engine runs were conducted with a configuration of 275 sensors (see figure 3a). The installation required every sensor and cable to be secured, prohibiting a rowing grid method.

performance and usability in a ground test campaign on aircraft [4]. The artificial excitation was realized using TIRA TV 51120-MOSP shakers with band-limited random excitation at 40-500 Hz. The measurement system used was a 480 (5x96) channel Simcenter SCADAS Mobile system, which controlled the excitation and was used to acquire time data. All further processing was done in custom software implemented in Matlab. More details regarding the general setup of the measurement system and the post-processing can be found in [2].

2.2. Experimental Structural Intensity Estimation

Structural Intensity (STI) is a vectoral quantity describing the vibrational power flow per unit areas through a structure. The STI is calculated by utilizing nodal velocities and rotations with the stresses acting in the elements. By multiplying the STI or the element stresses with the cross-sectional area in flow direction it is possible to acquire the power flow in the unit Watt directly. The power flow for plate elements in x- and y-direction while neglecting the z-direction (thickness of the plate) can be described by

$$P_{x,s} = -\frac{1}{2} Re \left\{ N_{x,s} v_x^* + N_{xy,s} v_y^* + M_{x,s} \omega_y^* + M_{xy,s} \omega_x^* + Q_{xz,s} v_z^* \right\} \tag{1}$$

and

$$P_{y,s} = -\frac{1}{2} Re \left\{ N_{y,s} v_y^* + N_{xy,s} v_x^* + M_{y,s} \omega_x^* + M_{xy,s} \omega_y^* + Q_{yz,s} v_z^* \right\}, \tag{2}$$

with N_i – normal element forces, M_i – element bending moments, Q_i – element transversal forces, v_i^* – complex conjugated nodal velocities, ω_i – nodal rotation speeds and the sub-index s indicating the values for shell elements [1]. All values and also the resulting intensities are time averaged and frequency dependent values. On the other hand, the power flow for beam elements can be described by

$$_b = -\frac{1}{2} Re \left\{ N_{x,b} v_x^* + T_b \omega_x^* - M_{y,b} \omega_y^* + M_{z,s} \omega_z^* + Q_{xz,b} v_z^* + Q_{xy,b} v_y^* \right\}, \tag{3}$$

with T_i – torsion along beam and the sub-index b indicating the values for beam elements [5].

In order to calculate the STI values it is necessary to have information regarding nodal translation and rotation quantities as well as the forces or tensions acting in the structure. While for FE models

this information are easily accessible because they can be calculated for the most complex of structures. However, when it comes to calculating STI values based on experimental data this becomes more difficult.

During experiments usually only, the outer velocity or acceleration field normal to the surface of structures can be measured. This means nodal rotations as well as tensions are missing to calculate the STI values. One commonly used approach is to calculate the structures tensions in discrete points by utilizing the Central Difference Method (CDM) which calculates the necessary derivatives of the displacement field by recursive operations [6]. This approach however has some drawbacks as it is only applicable on equidistant meshes, higher order derivatives result in progressing errors and there is a need for higher evaluation space as the higher order derivatives need several measurement points aligned.

An alternative method based on the utilization of the FEM process [7] overcomes these drawbacks and also makes it easy to extend the evaluation of structures for different element types. The measured field quantities are projected onto a mesh. With this approach the missing nodal rotations and element-based tensions can be calculated by using trial functions and the laws of elasticity for the elements which need to be evaluated.

Additionally, this approach allows to calculate STI fields for different elements based on the same field quantities acquired by measurements. For example, for lightweight structures which consists of bar-like frames covered with thin skins STI values can be calculated on shell elements representing the skins and on beam elements representing the frame. Overlaying the results of these two vector fields results in a combined STI field carrying more information.

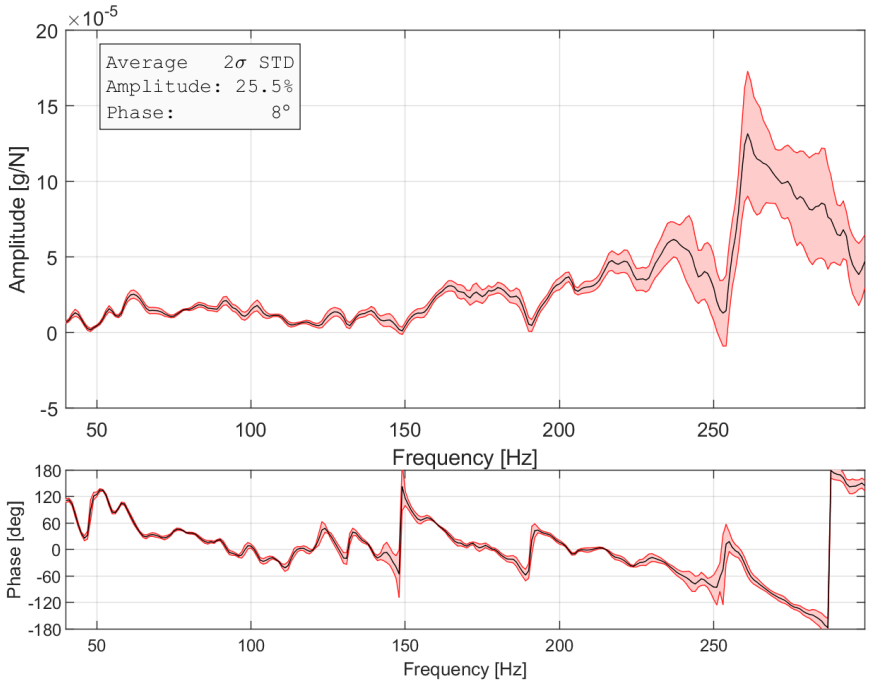

Figure 4: 2σ deviation of a sensor present during all 5 configurations (see figure 2b). This sensor is located at the middle of the fuselage and it's deviation in amplitude and phase representative for all fixed sensors.

3. RESULTS

3.1. Data consistency and quality

A drawback of the rowing grid is the risk of low data consistency. It has previously been shown not to be a problem (see [2, 3]) but needs to be checked after each measurement. To check the data, the sensors present during each grid configuration are evaluated. For this test these are the sensors shown in figure 2b. The 2σ standard deviation of the frequency response functions (FRF) is calculated for both amplitude and phase for the evaluated frequency range. This is shown for an exemplary sensor in figure 4. As the graph shows data consistency is quite good up to 200 Hz, larger deviations in the amplitude appear above this limit. The average 2σ amplitude deviation in a frequency range of 40 Hz to 300 Hz is 25.5%. This is mostly caused by including data above 200 Hz and consistent with what was observed in the past. The phase response deviation is similar in behavior, rising towards higher frequencies, with a 2σ deviation of 8°. Previous tests showed that this data should in principle be of sufficient quality for experimental modal analysis up to approximately 100 Hz. Updating the FEM of the ISTAR should be possible using this data. For the higher frequency range different methods need to be applied, like the energy correlation criterion [8].

3.2. Operational Deflection Shapes

All acquired data was processed into frequency domain and, in the case of artificial shaker excitation, frequency response functions (FRF) were estimated. For the engine measurements (see figure 3a) direct calculation of the spectral response was used instead, as no reference in form of a force cell is present. By plotting this data to the geometry the operational deflection shapes (ODS) are visualized. This is very useful, especially when animated, to get a quick impression of the data consistency and quality (see section 1 above).

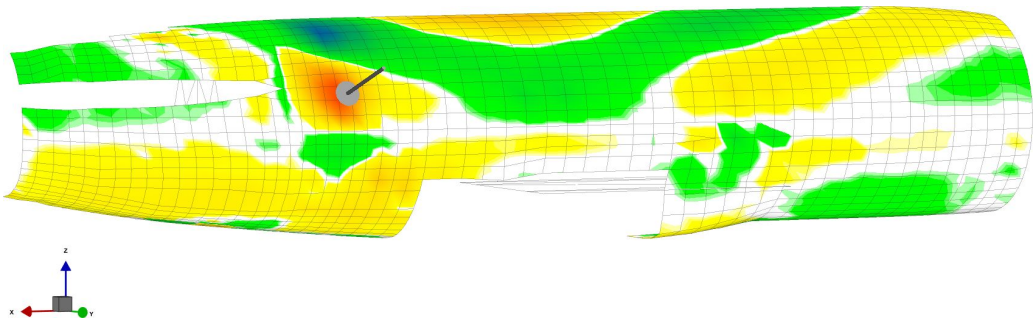

(a) ODS at 74 Hz for shaker excitation in Y direction. A dividing white horizontal line is visible. This is where the belly fairing begins.

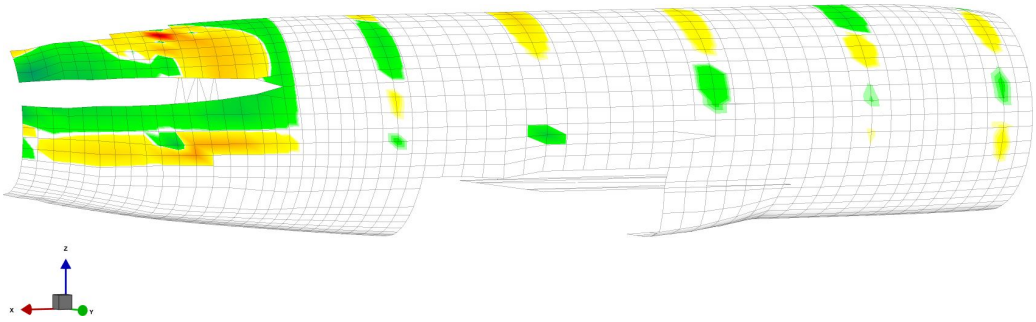

(b) ODS resulting from engine excitation at 74 Hz. The grid is dense around the pylon only.

Figure 5: Operational deflection shapes as the result of shaker and engine excitation.

Sample ODS are shown in 5a. The deflection shapes are smooth, confirming the observation made in section 1. In figure 5a a dividing line is clearly visible at the middle of the fuselage. This is where

the belly fairing is attached to the structure. The belly fairing of the Falcon 2000LX is a flexible composite structure and expected to show a behavior different to what the actual fuselage does. It was included in the measurements because the underlying structure was not accessible during the test. It remains to be seen up until which frequency range the data acquired on the belly fairing is of use. For the lower end of the data, 100 Hz and below, the belly fairing shows behavior consistent with what is happening on the primary structure.

3.3. Structural Intensity

One of the primary goals for the measurement campaign was the calculation of an experimental STI field. To be precise, the calculation of the divergent vector field, which should clearly show the existence of both energy sinks and sources. Figure 6 shows the structural intensity calculated directly from the ODS shown in figure 5a. At 74 Hz the vector field does show a lot of surprises, but the method clearly works. The shakers attachment point is easy to locate as a source of energy by the red cones. The energy mostly spreads out evenly from this point. A closer look at the vector field shows two

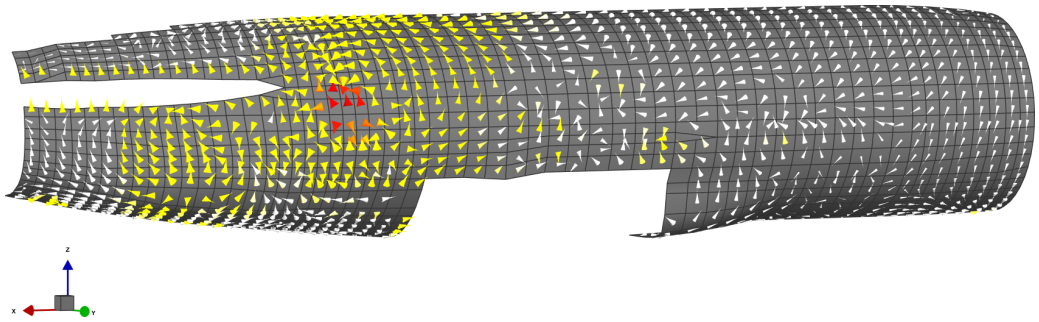

Figure 6: The divergent vector field of the STI calculated based on the ODS shown in figure 5a

.

oddities: There is energy flowing in at the front. Without any sensors at the other side of the fuselage we can only guess the source: The floor structure proofed to be an efficient path for energy transfer in previous measurements [3]. This could be one possible path of the energy reemerging on the of site of the aircraft. The second observation that can be made is, a secondary source clearly appears at the lower left side of the fuselage by a circle of cones pointing outward. At this point we can only speculate what is causing this: It is in line with the frame the pylon is attached to and the fuselage has a very steep curve at this point. It is also possible this source is an artifact caused by the belly fairing structure which ends at this point.

4. CONCLUSIONS AND NEXT STEPS

In a measurement campaign lasting two weeks vibration responses of the DLR ISTAR were acquired at 1350 positions. Additionally engine induced vibrations were measured at 275 positions. The data covers the low to mid-frequency range and is of sufficient quality for planned work in FE model updating. In addition first calculations of energy transfer paths using STI were conducted. These do not show a lot of surprises in the low frequency range, but that was mostly to be expected. The fact that the STI calculation is possible and showing a intuitively viable energy flow field proves the experimental data to be of good quality and sufficient spatial resolution.

An in depth analysis of the STI requires more work and will be done in the near future: The presented analysis rather arbitrarily picked the 74 Hz band. While it is a good representation for the structural behavior in the lower acoustic frequency regime, this was done purely by engineering judgement. The next steps include transfering the ODS shapes into principle ODS or PODS (see [3]) to get a mathematically representation of the structural behavior in wider frequency bands.

ACKNOWLEDGEMENTS

This project has received funding from the Clean Sky 2 Joint Undertaking under the European Union's Horizon 2020 research and innovation programme under grant agreement N° CS2-LPA-GAM-2020-2023-01.

REFERENCES

[1] Jörn Biedermann, Rene Winter, Marco Norambuena, and Marc Böswald. A hybrid numerical and experimental approach for structural intensity analysis of stiffened lightweight structures, 2018.

[2] René Winter, Jörn Biedermann, Marc Böswald, and Martin Wandel. Dynamic characterization of the A400M acoustics fuselage demonstrator, 2016.

[3] Rene Winter, Jörn Biedermann, and Marco Norambuena. High-resolution vibration measurement and analysis of the flight-lab aircraft fuselage demonstrator, 2018.

[4] Y. Govers, J. Sinske, and T. Petzsche. Latest design trends in modal accelerometers for aircraft ground vibration testing. *Sensors and Instrumentation, Aircraft/Aerospace, Energy Harvesting Dynamic Environments Testing, Vol 7*, pages 97–106, 2020.

[5] S. A. Hambric. Power flow and mechanical intensity calculations in structural finite-element analysis. *Journal of Vibration and Acoustics-Transactions of the Asme*, 112(4):542–549, 1990.

[6] E. G. Williams, H. D. Dardy, and R. G. Fink. A technique for measurement of structure-borne intensity in plates. *Journal of the Acoustical Society of America*, 78(6):2061–2068, 1985.

[7] F. Pires, S. Avril, S. Vanlanduit, and J. Dirckx. Structural intensity assessment on shells via a finite element approximation. *Journal of the Acoustical Society of America*, 145(1):312–326, 2019.

[8] Jörn Biedermann, René Winter, Martin Wandel, and Marc Böswald. Energy based correlation criteria in the mid-frequency range. *Journal of Sound and Vibration*, 400:457–480, 2017.